Applied Mechanics and Materials Vol. 553 (2014) pp 10-15
© (2014) Trans Tech Publications, Switzerland
doi:10.4028/www.scientific.net/AMM.553.10

Finite element modelling of stress-induced fracture in Ti-Si-N films

E.A. Flores-Johnson[1,a], L. Shen[1,b] , R.K. Annabattula[2,c], P.R. Onck[3,d], Y.G. Shen[4,e] and Z. Chen[5,6,f]

[1]School of Civil Engineering, The University of Sydney, Sydney, NSW 2006, Australia

[2]Department of Mechanical Engineering, Indian Institute of Technology Madras, Chennai, India

[3]Zernike Institute for Advanced Materials, University of Groningen, The Netherlands

[4]Department of Mechanical and Biomedical Engineering, City University of Hong Kong, Hong Kong

[5]Department of Civil and Environmental Engineering, University of Missouri, USA

[6]Department of Engineering Mechanics, Dalian University of Technology, China

[a]emmanuel.flores-johnson@sydney.edu.au, [b]luming.shen@sydney.edu.au,

[c]ratna@iitm.ac.in, [d]p.r.onck@rug.nl, [e]meshen@cityu.edu.hk, [f]chenzh@missouri.edu

Keywords: Thin film, buckling, cracking, finite element modelling.

Abstract. Nanocomposite coating films have been increasingly used in industrial applications because of their unique mechanical and physical properties. Residual stresses generated during the growth of sputter-deposited thin films due to a strain mismatch between the film and the substrate may lead to significant failure problems. Large residual stresses may generate buckling, delamination and film fracture. Although buckles with cracks in thin films have been experimentally observed, their origins are still not well understood.

In this work, finite element simulations in Abaqus/Explicit are employed to study buckling and cracking in Ti-Si-N films on a silicon substrate. Residual stresses in the film are generated using two loading methods: 1) Eigenstrain is applied via a temperature field; 2) An initial stress field is applied. Cracking is modelled using an elastic material model with a brittle fracture criterion that takes into account the tensile strength of the material to initiate damage.

It is found that while both loading methods lead to similar buckling patterns and stresses, an initial stress field generates premature film failure and thus the thermal field loading should be used. The numerical model fairly predicted the cracking patterns observed in the experiments.

Introduction

Nanocomposite coating films have been increasingly used in industrial applications such as high-speed machining, tooling, optical and magnetic storage devices because of their unique mechanical and physical properties [1]. TiN based thin films benefit from the combined attributes of individual components leading to a superior performance [2]. Adding small amounts of Si into TiN films produces a significant enhancement of hardness when compared with binary nitride TiN films [2]. In these types of films, maximum hardness (30-50 GPa) can be achieved at Si contents of 6-12% using magnetron sputtering techniques [3].

Residual stresses (tensile or compressive) are usually generated during the growth of sputter-deposited thin films [2]. The total residual stress in thin films mainly consists of a thermal stress and an intrinsic stress. The thermal stress is due to the difference in the thermal expansion coefficients of the film and substrate materials [4], while the intrinsic stress arises primarily from the process of film growth and epitaxy [5]. Large residual stresses may generate severe failure problems such as film and substrate cracking and film decohesion by buckling, which are detrimental to the integrity and performance of the films [4].

Buckling may initiate at imperfections or small interface separations in films subjected to residual compressive stresses [6]. Depending on several factors such as residual stresses, film

thickness and interface adhesion, delamination can localise and propagate across the film in a straight-sided buckle and/or a telephone cord buckle [7]. The film initially buckles as an axisymmetric buckle or circular blister referred to as the Euler buckling mode. With further increase in stresses, the initial buckle will evolve into a telephone cord shaped buckle. The film will have a transition buckling shaped called varicose between a blister and a telephone cord buckle [8].

Although there are several investigations dealing with the numerical modelling of buckling of hard films on Si substrates, modelling of Ti-Si-N films is limited. Furthermore, cracking on these films has not been investigated numerically and the origins of buckles with cracks reported experimentally are still not clear [2].

The motivation for this paper comes from the experimental observations of buckling and cracking of Ti-Si-N films reported by Liu et al [2], which are not fully understood. In this work, finite element simulations in Abaqus/Explicit are employed to study buckling and cracking in Ti-Si-N films on a silicon substrate. Residual stresses in the film are generated using two loading methods: 1) Eigenstrain is applied via temperature field; 2) An initial stress field is applied. Cracking is modelled using an elastic material model with a brittle fracture criterion that takes into account the tensile strength of the material. Numerical results are presented and discussed.

Problem definition and methodology

Buckling and cracking of Ti-Si-N thin films. Available experimental observations of buckling and cracking of $Ti_{0.39}$-$Si_{0.04}$-$N_{0.57}$ films deposited on Si(100) substrates reported in [2] are employed to validate the numerical simulations. The elastic and thermal material properties used for the film are shown in Table 1.

Table 1 Material properties of $Ti_{0.39}$-$Si_{0.04}$-$N_{0.57}$ film.

Material properties	$Ti_{0.39}$-$Si_{0.04}$-$N_{0.57}$
Density ρ (kg/m^3)	4900 [9]
Young's modulus E (GPa)	340 [9]
Poisson's ration ν (GPa)	0.25 [9]
Expansion coefficient α (K^{-1})	3.2x10^{-6} [4]
Tensile strength σ_T (GPa)	3.4

Finite element modelling. Numerical calculations of the buckling of thin films were carried out using a 3D finite element model built in Abaqus/Explicit [10] (Fig. 1). The film dimension was 25 × 75 μm^2 with a thickness of 0.7 μm [2]. The substrate is treated as a rigid body as experimental observations show no damage on the substrate surface [2]. Also, previous simulations have treated Si as rigid substrate when the Young's modulus of the substrate is larger than one fifth of that of the film [7], which is the case in this work (E≈170 GPa for Si(100) [11]). The element size in the film was 1 × 1 × 0.35 μm^3. Two elements were used through the film thickness giving a total of 3750 incompatible-modes linear hexahedral elements (C3D8I). Since the objective of this work is to study the postbuckling cracking, the substrate and the film are initially debonded and contact between the film and the substrate was taken into account by using the penalty contact algorithm available in Abaqus/Explicit and defining a coefficient of friction equal to zero [10]. An elastic material model was used to describe the behaviour of the film using the material properties shown in Table 1. Cracking is modelled using the *Brittle Cracking option in Abaqus that takes into account the tensile strength of the material to initiate damage in the elements [10]. A tensile strength of 3.4 GPa was used based on Pelton et al. [12], in which, it is stated that for TiN films the ultimate stress must be near the elastic limit at a deformation of approximately 1%.

When the Young's modulus of the substrate is at least one fifth of that of the film, confinement of a delamination buckle to a narrow strip can be assumed [7]. This buckling behaviour of a film detached from the substrate under compression stresses is modelled as a plate that is fully clamped along its edges [7].

The simulation comprises two main steps: i) an eigenvalue buckling analysis performed in Abaqus/standard. A superposition of mode shapes obtained from this analysis is used as imperfections (the amplitude of these imperfections is taken to be much smaller than the film thickness) in the next step to trigger the film buckling; and ii) a loading analysis performed in Abaqus/Explicit, in which, the film is loaded. Loading is achieved by increasing the temperature of the film until an eigenstrain of 1% is reached or by defining an initial stress field of 4.2 GPa equal to the reported residual stress in the film [2].

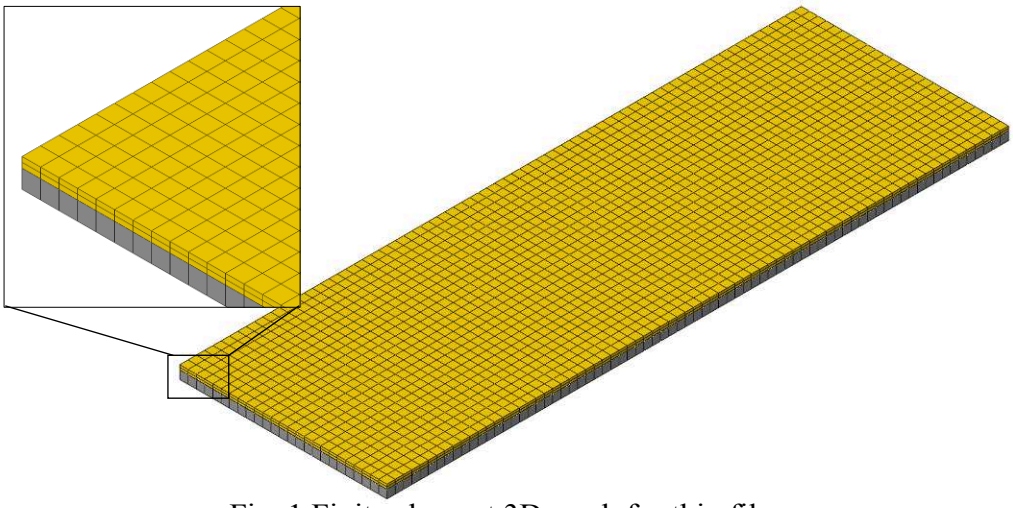

Fig. 1 Finite element 3D mesh for thin film.

Numerical results

Figure 2 shows contour plots of the out-of-plane deflection of the film at different eigenstrain. The evolution of the buckling with the increase of temperature (eigenstrain) shows the transition from the initial buckling to Euler mode, varicose mode and telephone-cord mode.

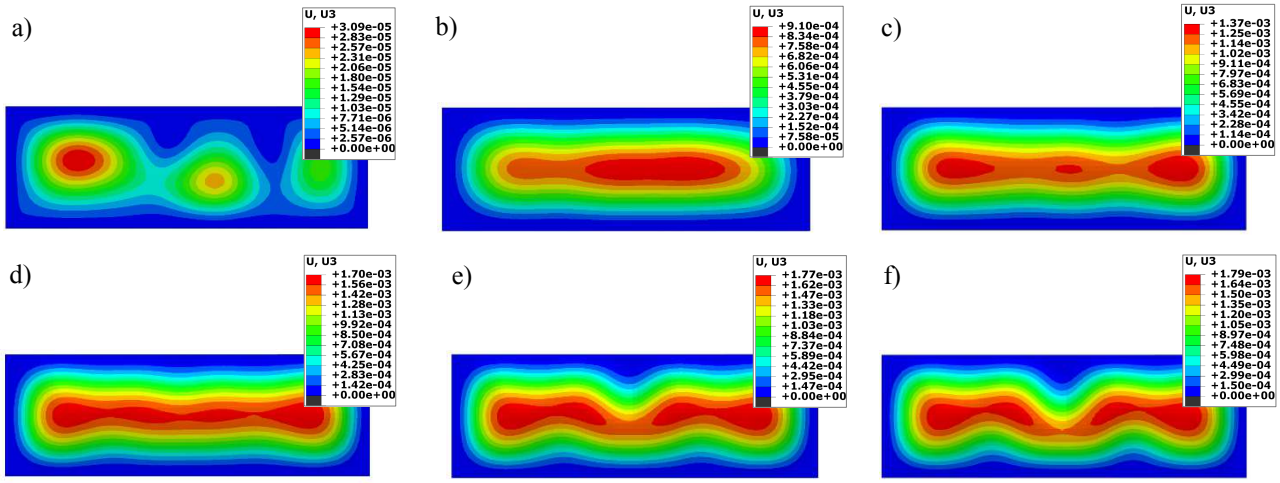

Fig. 2 Contour plots of the out-of-plane deflection of the film at different eigenstrain: a) ε^*=0.0011, b) ε^*=0.0033, c) ε^*=0.0063, d) ε^*=0.0092, e) ε^*=0.0099, f) ε^*=0.0103.

Figure 3 shows a comparison of the stress histories in the film by using both loading methods. Similar buckling pattern and maximum residual stress can be obtained when using either stress field

or temperature field loading. However, when the stress field loading method is used, a big jump (peak) in the stress is observed at the moment of the initial buckling, which is higher than the tensile strength. A series of stress peaks follow the initial stress peak until the system relaxes by buckling. The stress fluctuates initially and goes to a converged value after the system is fully relaxed. When no cracking is intended to be modelled, this method may not affect the results; however, for cracking modelling, temperature field should be used to avoid premature failure of the film due to the stress peaks.

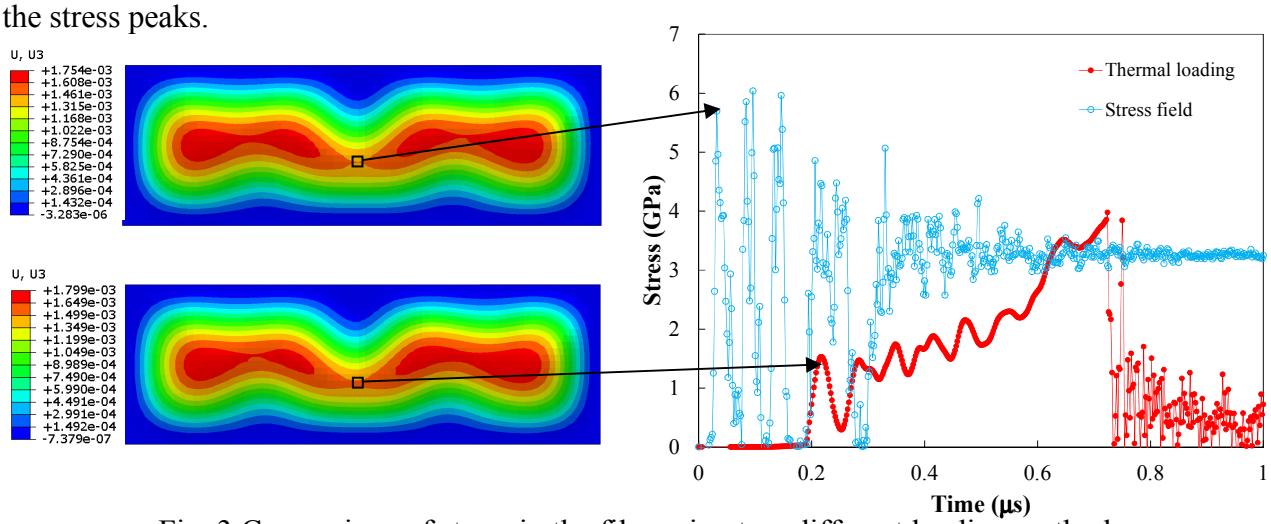

Fig. 3 Comparison of stress in the film using two different loading methods.

Figure 4 shows contour plots of the maximum principal stress in the film (Fig. 4a: Top view, Fig. 4b: Bottom view). A deformation scale factor of 10 is applied to the film in order to better visualise the stresses. It can be seen that the tensile stress in elements at the boundaries is higher than the tensile stress of those elements at the top of the buckle. This difference is due to the boundary constrains that have been imposed. It has been shown that film cracking may occur in either the apexes or the bottom of the buckles [13]; however, experimental observations show that in the case of the Ti-Si-N films used in this investigation [2], the stress is higher in the apexes. If the bending-induced stress at the apexes exceeds the flexural strength of the film, cracks will initiate; however, if the stresses are higher in the bottom part due to the artificial constrains, cracks will initiate there.

Two different approaches may be used to overcome this problem: 1) to define a failure criterion in all elements except those at the boundaries; 2) to use cohesive elements at the boundaries instead of fixed boundary conditions. In this work, the first approach will be used while second approach will be implemented in future work.

Figure 5 shows contour plots of the out-of-plane deflection of the film when a crack propagates in a telephone core buckle. It can be seen that the crack initiates at the apex of the buckle as observed experimentally [2], and then propagates toward the ends of the buckle. Figure 6 compares a crack observed in the experiment [2] with a crack obtained via numerical simulation. It can be seen that the predicted crack shape is fair; however, further work has to be done to accurately predict the cracking patterns. An improved fracture criterion and a finer mesh will be implemented in future work.

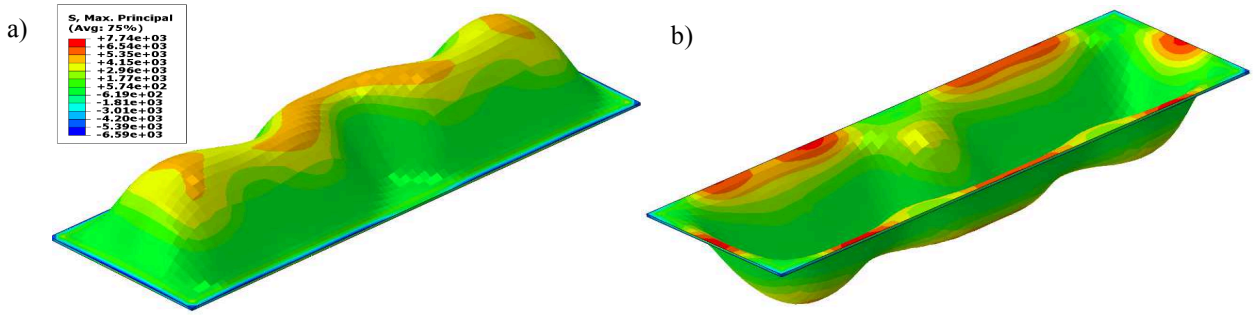

Fig. 4 Comparison of the maximum principal stresses in the film: a) top view, b) bottom view (A deformation scale factor of 10 is applied).

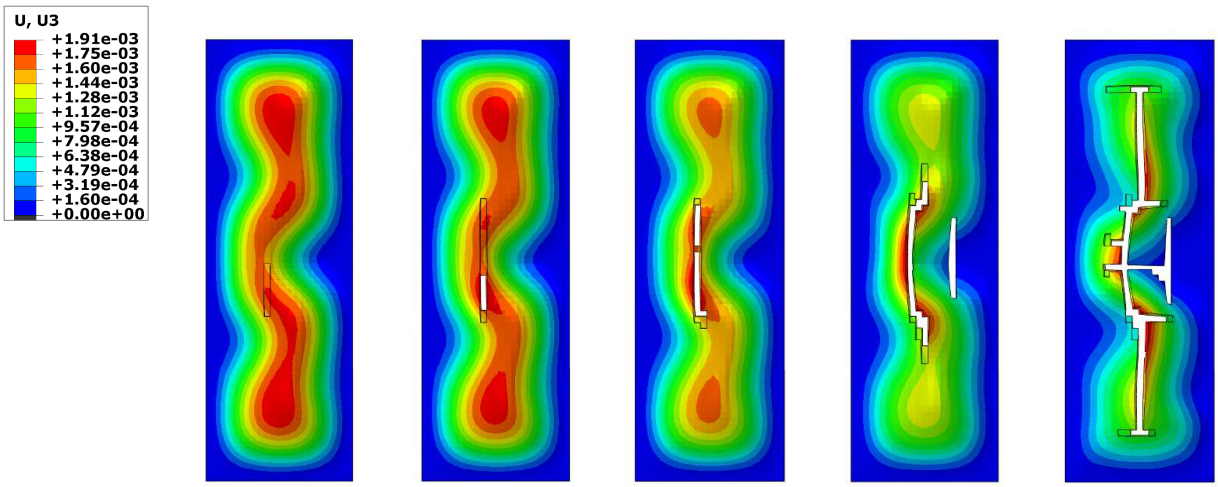

Fig. 5 Evolution of a crack in a telephone cord buckle (contour plots are out-of plane deflection).

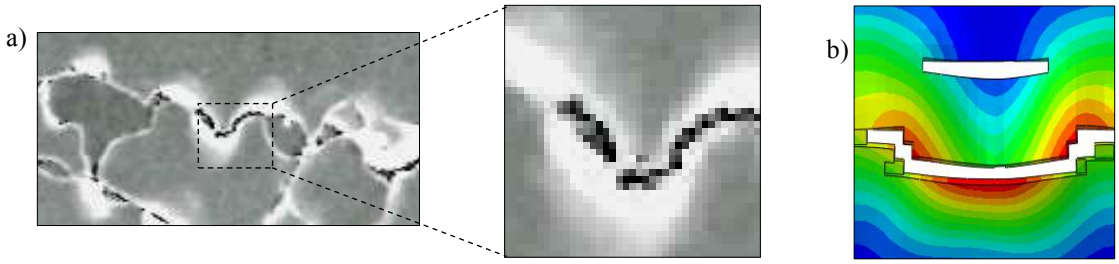

Fig. 6 Comparison of a crack in film a) experiment [2], b) simulation.

Summary

In this work, finite element simulations in Abaqus/Explicit are employed to study buckling and cracking in Ti-Si-N films on a silicon substrate. Residual stresses in the film are generated using two loading methods: 1) Eigenstrain is applied via temperature field; 2) An initial stress field is applied. Cracking is modelled using an elastic material model with a brittle fracture criterion that takes into account the tensile strength of the material.

It is found that while both loading methods lead to similar buckling patterns and stresses, an initial stress field will generate premature film failure and thus the thermal field loading should be used. The numerical model fairly predicted the cracking patterns observed in the experimental observations; however, further work has to be done to improve the model by using an improved fracture criterion and a finer mesh, which will be implemented in future work.

Acknowledgements

E.A. F-J. and L. S. acknowledge the partial financial support from the Australian Research Council (ARC) Centre of Excellence for Design in Light Metals (CE0561574).

References

[1] S. Zhang, D. Sun, Y. Fu, H. Du: Surf. Coat. Technol. Vol. 167 (2003) p. 113.

[2] Z.-J. Liu, N. Jiang, Y.G. Shen, X. Li: Thin Solid Films Vol. 516 (2008) p. 7609.

[3] Y.G. Shen, Z.-J. Liu, N. Jiang, H.S. Zhang, K.H. Chan, Z.K. Xu: J. Mater. Res. Vol. 19 (2004) p. 523.

[4] F. Vaz, L. Rebouta, Ph. Goudeau, J.P. Riviere, E. Schaffer, G. Kleer, M. Bodmann: Thin Solid Films Vol. 402 (2002) p. 195.

[5] L. Shen and Z. Chen: Model. Simul. Mater. Sci. Eng. Vol. 12 (2004) p. s347.

[6] M.-W. Moon, J.-W. Chung, K.-R. Lee, K.H. Oh, R. Wang, A.G. Evans: Acta Mater. Vol. 50 (2002) p. 1219.

[7] M.-W. Moon, K.-R. Lee, K.H. Oh, J.W. Hutchinson: Acta Mater. Vol. 52 (2004) p. 3151.

[8] R.K. Annabattula, P.R. Onck: J. Appl. Phys. Vol. 109 (2011) p. 033517.

[9] F. Vaz, S. Carvalho, L. Rebouta, M.Z. Silva, A. Paul, D. Schneider: Thin Solid Films Vol. 408 (2002) p. 160.

[10] Abaqus Analysis User's Manual (Version 6.11), SIMULIA (2011).

[11] R. Saha, W.D. Nix: Acta Mater. Vol. 50 (2002) p. 23.

[12] A.R. Pelton, B.W. Dabrowski, L.P. Lehman, C. Ernsberger, A.E. Miller, J.F. Mansfield: Ultramicroscopy Vol. 29 (1989) p. 50.

[13] J.S. Wang, A.G. Evans: Acta Mater. Vol. 47 (1999) p. 699.